

*Electronic Supplementary Information (ESI)*

**Control over synthesis of homovalent and mixed-valent cubic  
cobalt-imidazolate cages**

Liang Liang,<sup>‡b</sup> Dong Luo,<sup>‡a</sup> Tao Zuo,<sup>a</sup> Xiao-Ping Zhou,<sup>\*a</sup> and Dan Li<sup>\*a</sup>

<sup>a</sup> College of Chemistry and Materials Science, Jinan University, Guangzhou, Guangdong 510632, P. R. China.

<sup>b</sup> Department of Chemistry, Shantou University, Shantou, Guangdong 515063, P. R. China.

<sup>‡</sup> These authors contributed equally to this work.

E-mail: zhouxp@jnu.edu.cn, danli@jnu.edu.cn

## Experimental Section

**General Procedure:** Starting materials, reagents, and solvents were purchased from commercial sources (Alfa-Aesar, Sigma-Aldrich and TCI) and used without further purification. FT-IR spectra were measured using a Nicolet Avatar 360 FT-IR spectrophotometer. Mass spectra were acquired with a Q-TOF premier mass spectrometer with Nano-Acquity LC system and a Hexin mass spectrometry API-TOFMS II. UV-vis spectra were recorded by an Agilent 8453 UV-vis spectrophotometer (Agilent Technologies Co. Ltd., USA). Thermogravimetric analysis (TGA) was carried out in a nitrogen stream using Q50 TGA (TA) thermal analysis equipment with a heating rate of 10 °C min<sup>-1</sup>. Powder X-ray diffraction patterns (PXRD) of the bulk samples were measured on a Bruker D8 Advance diffractometer (Cu K $\alpha$ ,  $\lambda$ = 1.5418 Å) at room temperature. Elemental analyses were carried out with an Elementar vario EL Cube equipment. Magnetic properties were measured on a Quantum Design MPMS-7 SQUID magnetometer. Diamagnetic corrections were made with Pascal's constants for all the constituent atoms (Variable-temperature magnetic susceptibilities were measured at 2-300 K at 2000 Oe field. The AC magnetic susceptibilities were measured at 2-20 K at 0 and 1000 Oe field under 100 Hz and 997 Hz. Field dependence of the magnetization were measured at range of 0-8 T field at 2 K, 3 K and 4 K). Electrochemical measurements were performed on a CHI660E electrochemical workstation.

### Synthesis of cages 1a, 1b, and 2-4

**Synthesis of 1a:** A mixture of cobalt(II) nitrate hexahydrate (0.08 mmol, 23.3 mg), sodium bromide (0.20 mmol, 20.6 mg), 5-methyl-imidazole-4-carboxaldehyde (0.12 mmol, 13.2 mg), 4-bromo-benzylamine (0.12 mmol, 22.3 mg), and N,N-diethylformamide (DEF) / ethanol (EtOH) mixed solvent (2.5 mL, 4:1, v/v) was sealed in a Pyrex glass tube and heated in an oven at 120 °C for 72 hours and cooled to room temperature at a rate of 5 °C/h. Black green polyhedron-like crystals were collected by filtration and washed with diethyl ether 3 times, then dried in vacuum oven at 80 °C for 12 hours (32.7 mg, yield 75.9 % based on Co(NO<sub>3</sub>)<sub>2</sub>·6H<sub>2</sub>O). IR spectrum (KBr, pellets, cm<sup>-1</sup>): 3392(w), 2975(w), 2944(w), 2911(w), 2854(w), 2363(w), 1655(m), 1605(vs), 1490(s), 1442(w), 1408(m), 1384(w), 1347(m), 1292(m), 1269(s), 1217(w), 1201(w), 1149(m), 1108(w), 1071(m), 1011(m), 980(w), 857(m), 830(m), 794(m), 709(w), 682(w), 643(w), 583(m), 526.29(w), 494(m), 469(w). Elemental analysis (CHN), C<sub>149</sub>H<sub>153</sub>Br<sub>16</sub>Co<sub>8</sub>N<sub>37</sub>O<sub>6</sub>, (corresponding to [Co<sup>II</sup><sub>8</sub>(L1)<sub>12</sub>Br<sub>4</sub>]·DEF·5H<sub>2</sub>O), calculated (%): C 41.54, H 3.58, N 12.03; found (%): C 41.31, H 3.56, N 12.02.

**Synthesis of 1b:** A mixture of cobalt(II) nitrate hexahydrate (0.08 mmol, 23.3 mg), sodium bromide (0.20 mmol, 20.6mg), 5-methyl-imidazole-4-carboxaldehyde (0.12 mmol, 13.2 mg), 4-bromo-benzylamine (0.12 mmol, 22.3mg), and DEF/EtOH mixed solvent (2.5 mL, 1:2, v/v) was sealed in a Pyrex glass tube and heated in an oven at 120 °C for 72 hours and cooled to room temperature at a rate of 5 °C/h. Black green block-like crystals were collected by filtration and washed with diethyl ether 3 times, then dried in vacuum oven at 80 °C for 12 hours (35.2 mg, yield 76.4 % based on Co(NO<sub>3</sub>)<sub>2</sub>·6H<sub>2</sub>O). IR spectrum (KBr, pellets, cm<sup>-1</sup>): 3401(m), 3019(w), 2974(w), 2947(w), 2912(w), 2852(w), 1605(vs), 1490(s), 1442(w), 1408(m), 1384(m), 1346(m), 1292(m), 1270(w), 1217(w), 1201(w), 1149(m), 1072(m), 1011(m), 979(w), 857(m), 830(m), 795(m), 682(w), 643(w), 583(m), 527(w), 494(w), 468(w). Elemental analysis (CHN), C<sub>149</sub>H<sub>153</sub>Br<sub>19</sub>Co<sub>8</sub>N<sub>38</sub>O<sub>9</sub>, (corresponding to [Co<sup>III</sup><sub>4</sub>Co<sup>II</sup><sub>4</sub>(L1)<sub>12</sub>Br<sub>4</sub>]·3Br·NO<sub>3</sub>·DEF·5H<sub>2</sub>O), calculated (%): C 38.82, H 3.35, N 11.55; found (%):

C 38.84, H 3.39, N 11.67. API-TOF MS:  $[\text{Co}_8(\text{L1})_{12}\text{Br}_4]\cdot\text{NO}_3^{3+}$ , m/z (maximum isotope peak): simulated 1392.42, observed 1392.43;  $[\text{Co}_8(\text{L1})_{12}\text{Br}_4]\cdot\text{Br}^{3+}$ , m/z (maximum isotope peak): simulated 1355.73, observed 1398.71;  $[\text{Co}_8(\text{L1})_{12}\text{Br}_4]\cdot 2\text{NO}_3^{2+}$ , m/z (maximum isotope peak): simulated 2120.64, observed 2120.60;  $[\text{Co}_8(\text{L1})_{12}\text{Br}_4]\cdot\text{Br}\cdot\text{NO}_3^{2+}$ , m/z (maximum isotope peak): simulated 2129.10, observed 2129.08;  $[\text{Co}_8(\text{L1})_{12}\text{Br}_4]\cdot 2\text{Br}^{2+}$ , m/z (maximum isotope peak): simulated 2137.57, observed 2137.51.

**Synthesis of 2:** A mixture of cobalt(II) nitrate hexahydrate (0.08 mmol, 23.3 mg), sodium bromide (0.20 mmol, 20.6 mg), 5-methyl-imidazole-4-carboxaldehyde (0.12 mmol, 13.2 mg), 4-fluorobenzylamine (0.12 mmol, 15.0mg), and DEF/EtOH mixed solvent (2.5 mL, 4:1, v/v) was sealed in a Pyrex glass tube and heated in an oven at 120 °C for 72 hours and cooled to room temperature at a rate of 5 °C/h. Black green polyhedron-like crystals were collected by filtration and washed with diethyl ether 3 times, then dried in vacuum oven at 80 °C for 12 hours (27.7 mg, yield 74.4 % based on  $\text{Co}(\text{NO}_3)_2\cdot 6\text{H}_2\text{O}$ ). IR spectrum (KBr, pellets,  $\text{cm}^{-1}$ ): 3421(m), 3122(w), 2976(w), 2915(w), 2854(w), 1658(w), 1608(vs), 1510(s), 1492(s), 1444(w), 1409(w), 1384(w), 1346(m), 1295(w), 1224(s), 1149(m), 1101(w), 1067(w), 1016(w), 980(w), 858(m), 823(m), 762(w), 682(w), 651(w), 602(m), 539(w), 510(w), 472(w), 461(w). Elemental analysis (CHN),  $\text{C}_{146.5}\text{H}_{167.5}\text{Br}_4\text{Co}_8\text{F}_{12}\text{N}_{36.5}\text{O}_{15.5}$ , (corresponding to  $[\text{Co}^{\text{II}}_8(\text{L2})_{12}\text{Br}_4]\cdot 0.5\text{DEF}\cdot 15\text{H}_2\text{O}$ ), calculated (%): C 47.47, H 4.55, N 13.79; found (%): C 47.18, H 4.31, N 13.94.

**Synthesis of 3:** A mixture of cobalt(II) nitrate hexahydrate (0.08 mmol, 23.3mg), sodium bromide (0.20 mmol, 20.6mg), 5-methyl-imidazole-4-carboxaldehyde (0.12 mmol, 13.2mg), 4-methylbenzylamine (0.12 mmol, 14.5mg), and DEF/EtOH mixed solvent (2.5 mL, 1:2, v/v) was sealed in a Pyrex glass tube and heated in an oven at 120 °C for 72 hours and cooled to room temperature at a rate of 5 °C/h. Black green block-like crystals were collected by filtration and washed with diethyl ether 3 times, then dried in vacuum oven at 80 °C for 12 hours (24.3 mg, yield 63.7 % based on  $\text{Co}(\text{NO}_3)_2\cdot 6\text{H}_2\text{O}$ ). IR spectrum (KBr, pellets,  $\text{cm}^{-1}$ ): 3400(m), 3122(w), 3019(w), 2976(w), 2947(w), 2914(w), 2855(w), 2377(w), 1901(w), 1662(w), 1609(vs), 1514(m), 1492(s), 1443(m), 1402(w), 1383(m), 1293(m), 1201(w), 1149(s), 1065(m), 1043(w), 981(m), 851(m), 838(m), 802(m), 751(w), 683(m), 650(m), 604(s), 540(w), 507(w), 481(m), 460(m). Elemental analysis (CHN),  $\text{C}_{161}\text{H}_{182}\text{Br}_7\text{Co}_8\text{N}_{38}\text{O}_{5.5}$ , (corresponding to  $[\text{Co}^{\text{III}}_4\text{Co}^{\text{II}}_4(\text{L3})_{12}\text{Br}_4]\cdot 3\text{Br}\cdot\text{NO}_3\cdot\text{DEF}\cdot 1.5\text{H}_2\text{O}$ ), calculated (%): C 51.32, H 4.87, N 14.12; found (%): C 51.35, H 4.57, N 14.58. API-TOF MS:  $[\text{Co}_8(\text{L3})_{12}\text{Br}_4]\cdot\text{NO}_3^{3+}$ , m/z (maximum isotope peak): simulated 1133.52, observed 1133.40;  $[\text{Co}_8(\text{L3})_{12}\text{Br}_4]\cdot\text{Br}^{3+}$ , m/z (maximum isotope peak): simulated 1139.16, observed 1139.07;  $[\text{Co}_8(\text{L3})_{12}\text{Br}_4]\cdot 2\text{NO}_3^{2+}$ , m/z (maximum isotope peak): simulated 1731.27, observed 1731.16;  $[\text{Co}_8(\text{L3})_{12}\text{Br}_4]\cdot\text{Br}\cdot\text{NO}_3^{2+}$ , m/z (maximum isotope peak): simulated 1740.23, observed 1740.13;  $[\text{Co}_8(\text{L3})_{12}\text{Br}_4]\cdot 2\text{Br}^{2+}$ , m/z (maximum isotope peak): simulated 1749.20, observed 1749.09.

**Synthesis of 4:** A mixture of cobalt(II) nitrate hexahydrate (0.08 mmol, 23.3 mg), sodium bromide (0.20 mmol, 20.6 mg), 5-methyl-imidazole-4-carboxaldehyde (0.12 mmol, 13.2 mg), 4-trifluoromethyl-benzylamine (0.12 mmol, 21.0 mg), and DEF/EtOH mixed solvent (2.5 mL, 1:2, v/v) was sealed in a Pyrex glass tube and heated in an oven at 120 °C for 72 hours and cooled to room temperature at a rate of 5 °C/h. Black green powder was collected by filtration and washed with diethyl ether 3 times (crude product, 32.6 mg). The crude product was dissolved in DMF (30 mL), and then the product was isolated as black green block-like crystals by slow vapor diffusion of diethyl ether into the solution of powder after one week (22.6 mg, yield 52.0 % based on  $\text{Co}(\text{NO}_3)_2\cdot 6\text{H}_2\text{O}$ ). IR spectrum (KBr, pellets,  $\text{cm}^{-1}$ ): 3674(w), 3413(m), 3123(w), 2984(w), 2952(w),

2916(w), 2856(w), 2698(w), 2645(w), 2379(w), 1925(w), 1662(m), 1604(vs), 1493(s), 1444(m), 1419(m), 1384(w), 1324(vs), 1171(s), 1114(s), 1067(s), 1018(m), 981(s), 860(s), 841(m), 817(m), 759(w), 728(w), 683(w), 648(s), 595(m), 537(w), 495(m). Elemental analysis (CHN),  $C_{157.5}H_{137.5}Br_7Co_8F_{36}N_{37.5}O_{4.5}$ , (corresponding to  $[Co^{III}_4Co^{II}_4(L4)_{12}Br_4] \cdot 3Br \cdot NO_3 \cdot 0.5DMF \cdot H_2O$ ), calculated (%): C 43.57, H 3.19, N 12.10; found (%): C 43.82, H 3.13, N 12.12. ESI-TOF MS:  $[Co_8(L4)_{12}Br_4] \cdot NO_3]^{3+}$ , m/z (maximum isotope peak): simulated 1349.40, observed 1349.54;  $[Co_8(L4)_{12}Br_4] \cdot Br]^{3+}$ , m/z (maximum isotope peak): simulated 1355.05, observed 1355.04;  $[Co_8(L4)_{12}Br_4] \cdot 2NO_3]^{2+}$ , m/z (maximum isotope peak): simulated 2055.10, observed 2055.33;  $[Co_8(L4)_{12}Br_4] \cdot Br \cdot NO_3]^{2+}$ , m/z (maximum isotope peak): simulated 2064.07, observed 2064.30;  $[Co_8(L4)_{12}Br_4] \cdot 2Br]^{2+}$ , m/z (maximum isotope peak): simulated 2073.03, observed 2073.02.

## Crystal Structure Analysis and Additional Characterization Crystallographic studies

### General:

Single crystal structures of **1a**, **1b**, **2**, **3**, and **4** were measured by X-ray diffraction. Data collection were performed on an Agilent Technologies Gemini A System (Cu K $\alpha$ ,  $\lambda$ = 1.54178 Å; Mo K $\alpha$ ,  $\lambda$ = 0.71073 Å). Crystals of **1a** to **4** were measured at 100 K. The data were processed using CrysAlis<sup>Pro.1</sup>. The structures were solved by direct methods and refined by full-matrix least-squares refinements based on  $F^2$ . Anisotropic thermal parameters were applied to all non-hydrogen atoms. The hydrogen atoms were generated geometrically. The crystallographic calculations were conducted using SHELXL-2018/3 program.<sup>S1</sup> All the crystal structures contain lots of unknown residual electron density belong to guest molecules and/or counter anions. The treatment for the guest molecules and partial free counter anions in the cavities involves the use of the SQUEEZE program of PLATON,<sup>S2</sup> which can provide a better refinement data. In addition, based on the instability and complexity of these crystals, the crystal structure data only can be obtained under cryogenic temperature (100 K). A summary of crystal data and structure refinement parameters is listed in Tables S1 and Table S2.

### Crystal refinement details:

**1a:** There is a benzene group (containing C7, C8, C9, C10, C11, C12) in the cage that is disordered with large thermal motion. SIMU instruction is used to restrain thermal parameter of these atoms and AFIX instruction is used to constrain these atoms in the same plane. The residual electron density per unit cell is 548 electrons, which may correspond to 4 DEF, 4 EtOH and 22 H<sub>2</sub>O guest molecules.

**1b:** The residual electron density per unit cell is 729 electrons, which may correspond to 4 NO<sub>3</sub><sup>-</sup>, 4 DEF, 6 EtOH and 22 H<sub>2</sub>O guest molecules.

**2:** The residual electron density per unit cell is 572 electrons, which may correspond to 2 DEF, 5 EtOH and 33 H<sub>2</sub>O guest molecules.

**3:** The residual electron density per unit cell is 179 electrons, which may correspond to 4 NO<sub>3</sub><sup>-</sup>, EtOH and 2.5 H<sub>2</sub>O guest molecules.

**4:** The terminal -CF<sub>3</sub> groups in the ligands have large thermal motion that DFIX, SIMU and EADP instruction are used to restrain thermal parameter of these atoms. The residual electron density per unit cell is 5963 electrons, which may correspond to 64 DMF, 77 Et<sub>2</sub>O and 17 H<sub>2</sub>O guest molecules. The reported crystal structure of cage **4** in this work is obtained accidentally and has poor reproducibility. Therefore, based on CHN data and ESI-TOF MS, the reasonable chemical formula of activated cage **4** is [Co<sup>III</sup><sub>4</sub>Co<sup>II</sup><sub>4</sub>(L4)<sub>12</sub>Br<sub>4</sub>] $\cdot$ 3Br $\cdot$ NO<sub>3</sub> $\cdot$ 0.5DMF $\cdot$ H<sub>2</sub>O.

<sup>S1</sup> (a) G. M. Sheldrick, Acta Crystallogr., Sect. A: Found. Crystallogr., 2008, **64**, 112. (b) C. B. Hubschle, G. M. Sheldrick and B. Dittrich, J. Appl. Cryst., 2011, **44**, 1281. (c) G. M. Sheldrick, Acta Cryst., 2015, **C71**, 3.

<sup>S2</sup> A. L. Spek, Acta Cryst., 2015, **C71**, 9.

**Table S1.** Summary of the Crystal Data and Structure Refinement Parameters for **1a**, **1b** and **2**

Parameter	<b>1a</b>	<b>1b</b>	<b>2</b>
Chemical Formula	C <sub>158</sub> H <sub>188</sub> Br <sub>16</sub> Co <sub>8</sub> N <sub>38</sub> O <sub>15</sub>	C <sub>162</sub> H <sub>185</sub> Br <sub>19</sub> Co <sub>8</sub> N <sub>40</sub> O <sub>13</sub>	C <sub>154</sub> H <sub>193</sub> Br <sub>4</sub> Co <sub>8</sub> F <sub>12</sub> N <sub>37</sub> O <sub>21</sub>
Formula Weight	4609.42	4890.15	3403.94
Temp (K)	100	100	100
Crystal System	<i>cubic</i>	<i>monoclinic</i>	<i>cubic</i>
Space Group	<i>P-43n</i>	<i>C2/c</i>	<i>P-43n</i>
<i>a</i> (Å)	21.5387(3)	30.59463(19)	21.0860(2)
<i>b</i> (Å)	21.5387(3)	19.52250(12)	21.0860(2)
<i>c</i> (Å)	21.5387(3)	33.3193(2)	21.0860(2)
<i>α</i> (deg)	90	90	90
<i>β</i> (deg)	90	110.4609(7)	90
<i>γ</i> (deg)	90	90	90
<i>V</i> (Å <sup>3</sup> )	9992.1(4)	18645.5(2)	9375.2(3)
<i>Z</i>	2	4	2
<i>D</i> <sub>calcd</sub> (g/cm <sup>3</sup> )	1.532	1.742	1.388
<i>μ</i> (mm <sup>-1</sup> )	9.192	10.652	6.911
Reflections Collected	8052	42411	12346
Unique Reflections	2802	18964	3008
<i>R</i> <sub>int</sub>	0.0719	0.0294	0.0417
<i>R</i> <sub>1</sub> [ <i>I</i> >2σ( <i>I</i> )] <sup>a</sup>	0.0837	0.0730	0.0619
<i>wR</i> <sub>2</sub> [ <i>I</i> >2σ( <i>I</i> )] <sup>b</sup>	0.2265	0.2133	0.1828
<i>R</i> <sub>1</sub> (all data) <sup>a</sup>	0.1776	0.0751	0.0675
<i>wR</i> <sub>2</sub> (all data) <sup>b</sup>	0.2850	0.2153	0.1860
GOOF	1.009	1.038	1.148
<i>F</i> (000)	4048	8964	3444
CCDC number	1872745	1872746	1872747

$$^a R_1 = \sum(|F_0| - |F_c|) / \sum|F_0|; \quad ^b wR_2 = [\sum w(F_0^2 - F_c^2)^2 / \sum w(F_0^2)^2]^{1/2}$$

**Table S2.** Summary of the Crystal Data and Structure Refinement Parameters for **3** and **4**.

Parameters	<b>3</b>	<b>4</b>
Chemical Formula	C <sub>166.5</sub> H <sub>194.1</sub> Br <sub>7</sub> Co <sub>8</sub> N <sub>39</sub> O <sub>3.9</sub>	C <sub>218.5</sub> H <sub>132</sub> Br <sub>13</sub> Co <sub>10</sub> F <sub>36</sub> N <sub>44</sub> O <sub>19.75</sub>
Formula Weight	3798.37	6001.76
Temp (K)	100	100
Crystal System	<i>monoclinic</i>	<i>orthorhombic</i>
Space Group	<i>C2/c</i>	<i>Fddd</i>
<i>a</i> (Å)	30.5517(18)	24.0922(19)
<i>b</i> (Å)	19.0256(7)	30.1286(12)
<i>c</i> (Å)	35.950(2)	68.447(3)
<i>α</i> (deg)	90	90
<i>β</i> (deg)	120.657(8)	90
<i>γ</i> (deg)	90	90
<i>V</i> (Å <sup>3</sup> )	17976(2)	49683(5)
<i>Z</i>	4	8
<i>D</i> <sub>calcd</sub> (g/cm <sup>3</sup> )	1.404	1.605
<i>μ</i> (mm <sup>-1</sup> )	7.929	8.142
Reflections Collected	37292	31574
Unique Reflections	18089	12276
<i>R</i> <sub>int</sub>	0.0576	0.1109
<i>R</i> <sub>1</sub> [ <i>I</i> >2σ( <i>I</i> )] <sup>a</sup>	0.1238	0.1405
<i>wR</i> <sub>2</sub> [ <i>I</i> >2σ( <i>I</i> )] <sup>b</sup>	0.3519	0.3732
<i>R</i> <sub>1</sub> (all data) <sup>a</sup>	0.1364	0.2629
<i>wR</i> <sub>2</sub> (all data) <sup>b</sup>	0.3665	0.4544
GOOF	1.483	1.210
<i>F</i> (000)	7756	18952
CCDC number	1872748	1872749

$$^a R_1 = \sum(|F_0| - |F_c|) / \sum|F_0|; \quad ^b wR_2 = [\sum w(F_0^2 - F_c^2)^2 / \sum w(F_0^2)^2]^{1/2}$$

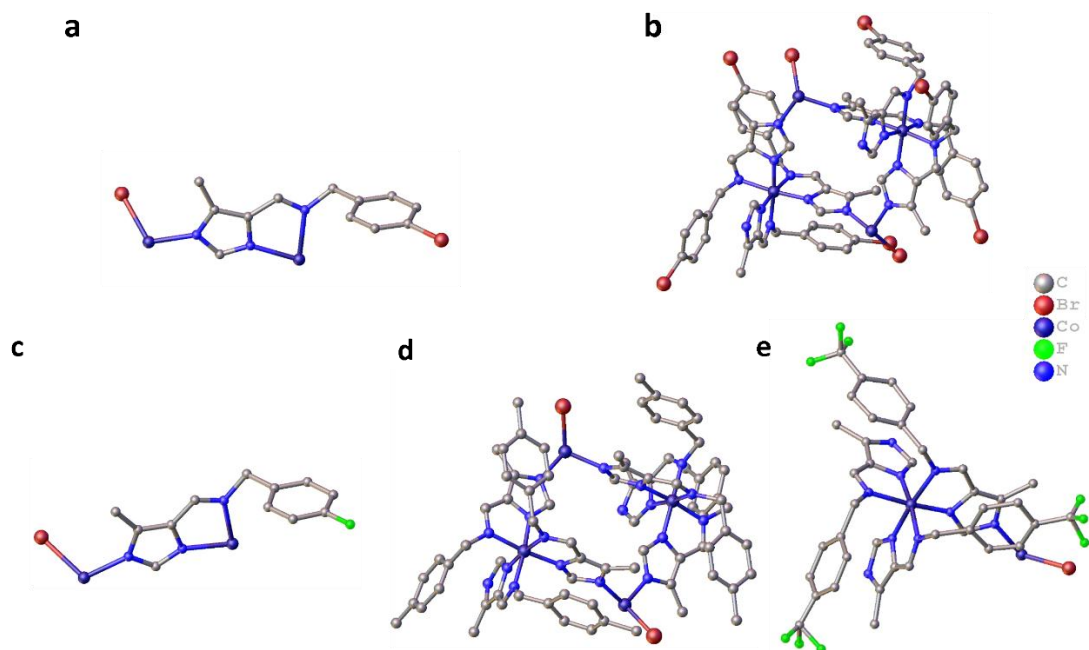


**Fig. S1** The asymmetric units of Co-imidazolate cubic cages **1a** (a), **1b** (b), **2** (c), **3** (d) and **4** (e). Color codes for elements: Co dark blue, N blue, C gray, Br red, F green, H atoms are omitted for clarity.

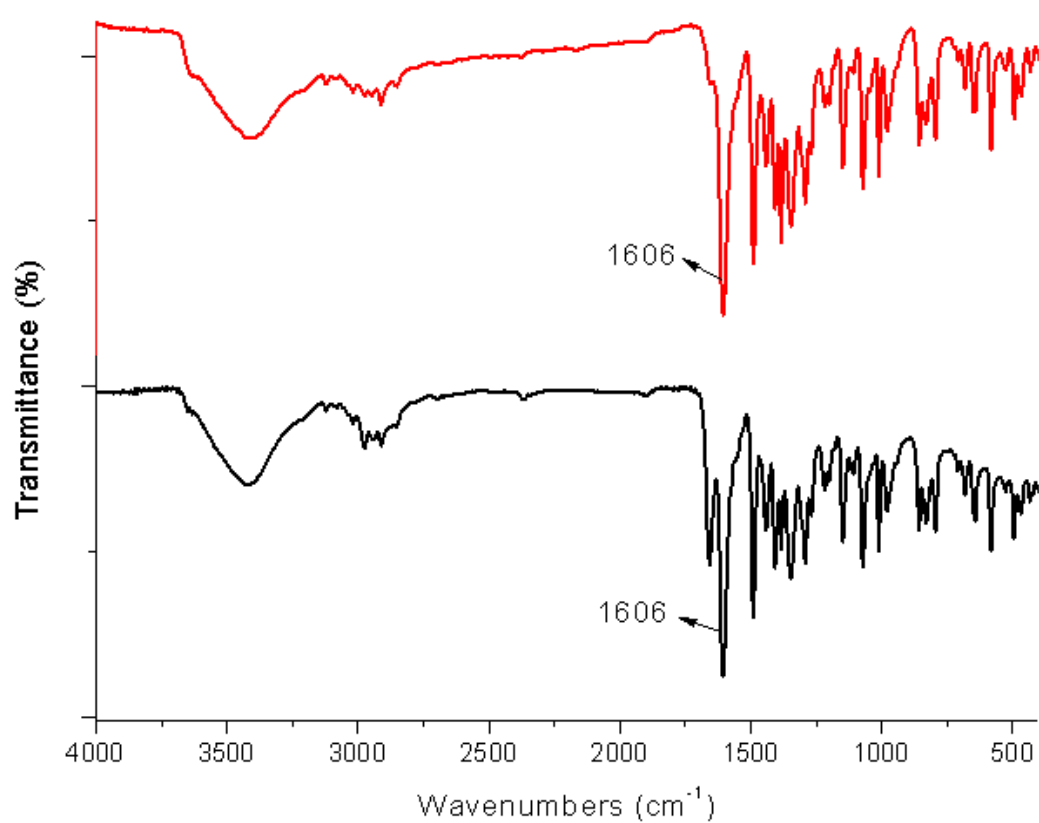


Fig. S2 The IR spectra of cage **1a** (black) and **1b** (red).

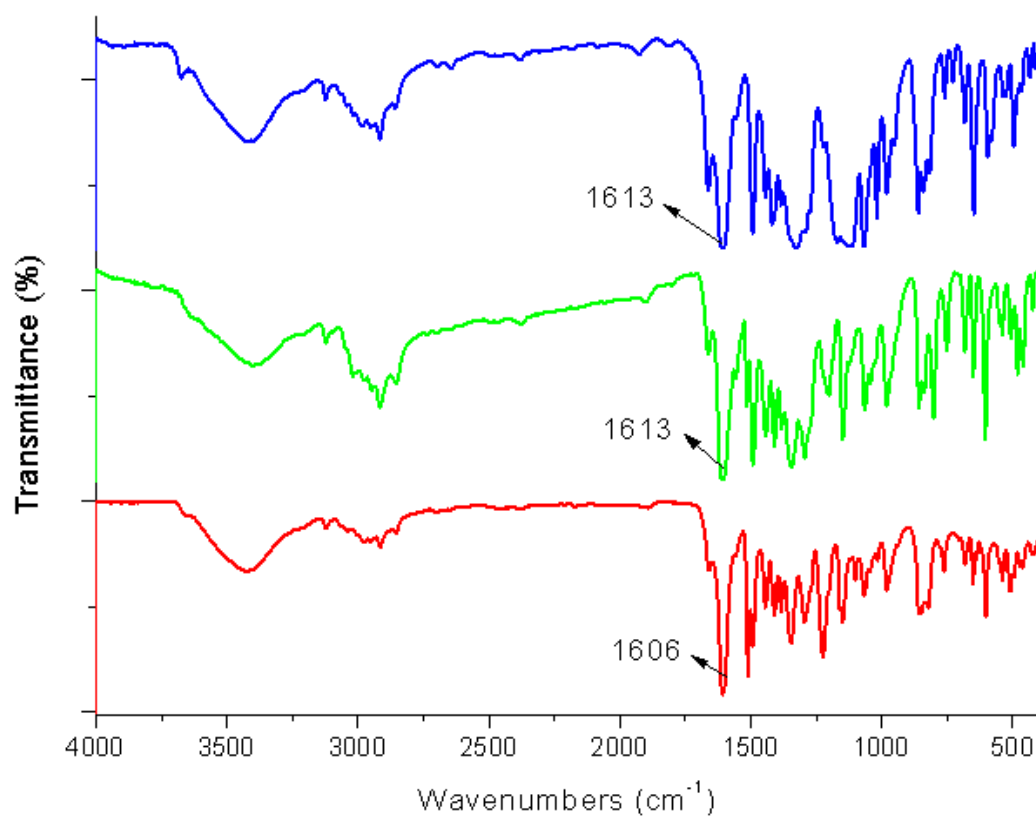
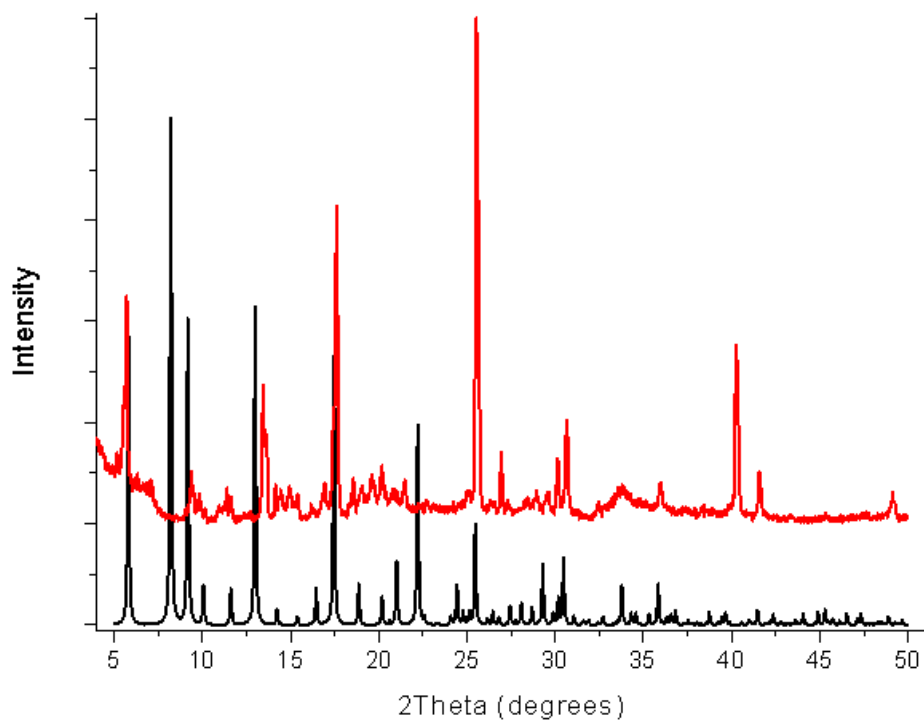
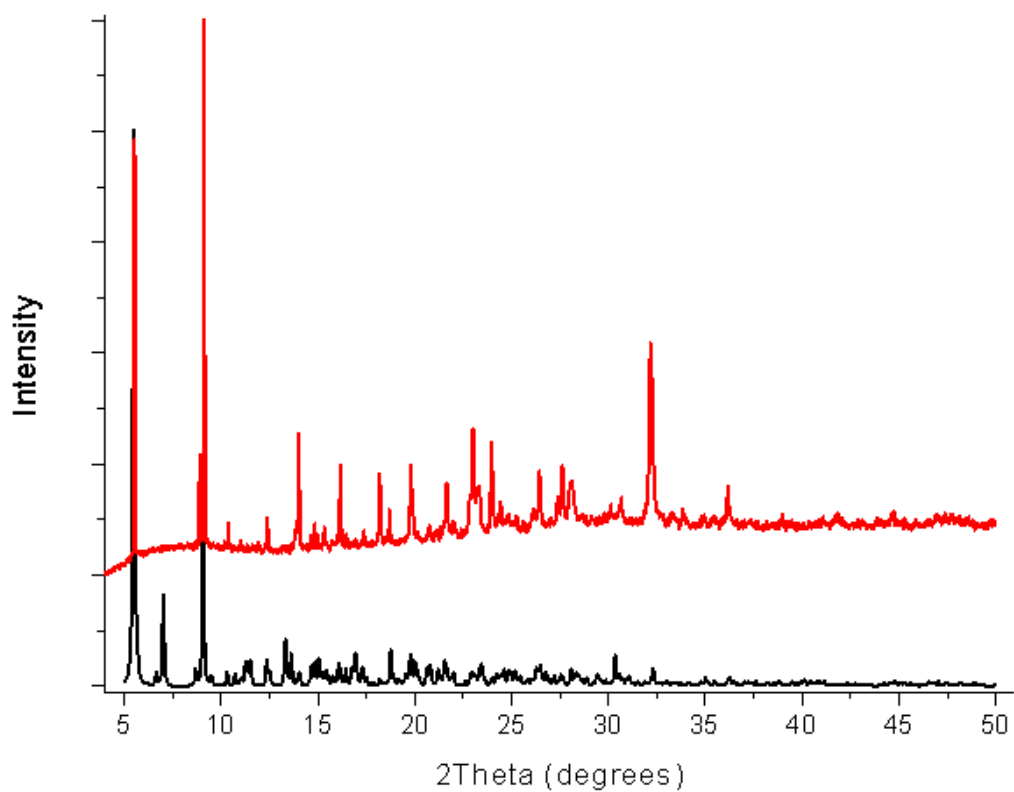


Fig. S3 The IR spectra of complexes **2** (red), **3** (green) and **4** (blue).



**Fig. S4** PXRD patterns of simulated (black) and as-synthesized (red) samples of **1a**.



**Fig. S5** PXRD patterns of simulated (black) and as-synthesized (red) samples of **1b**.

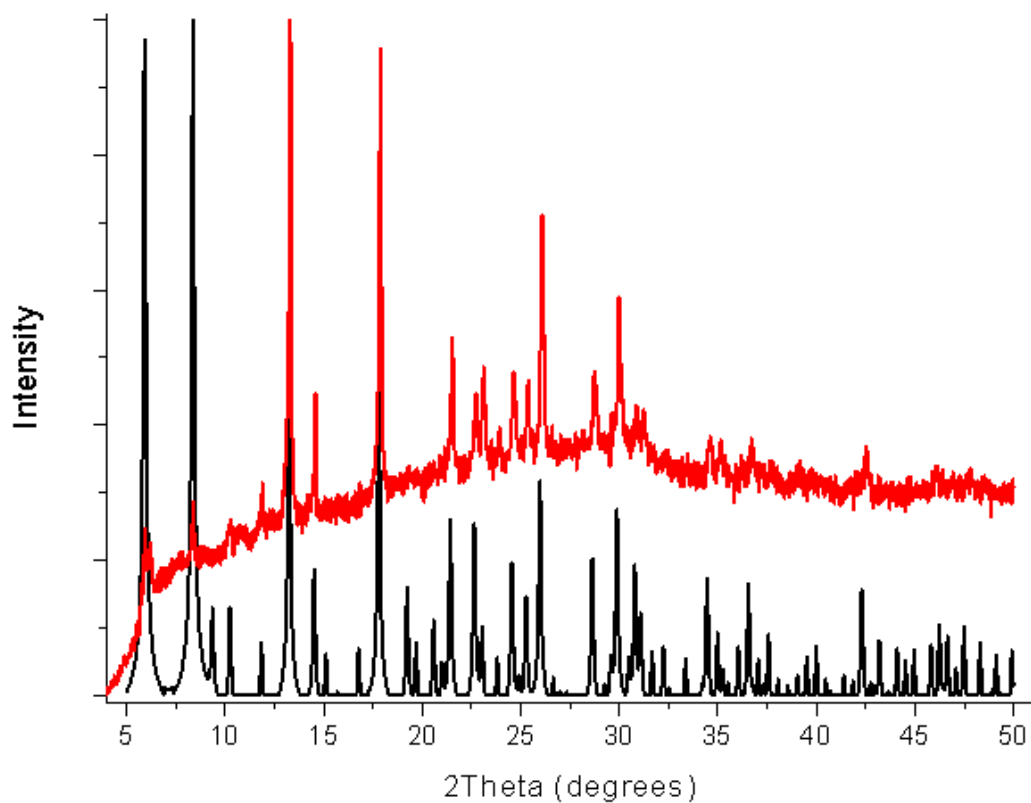


**Fig. S6** PXRD patterns of simulated (black) and as-synthesized (red) samples of **2**.

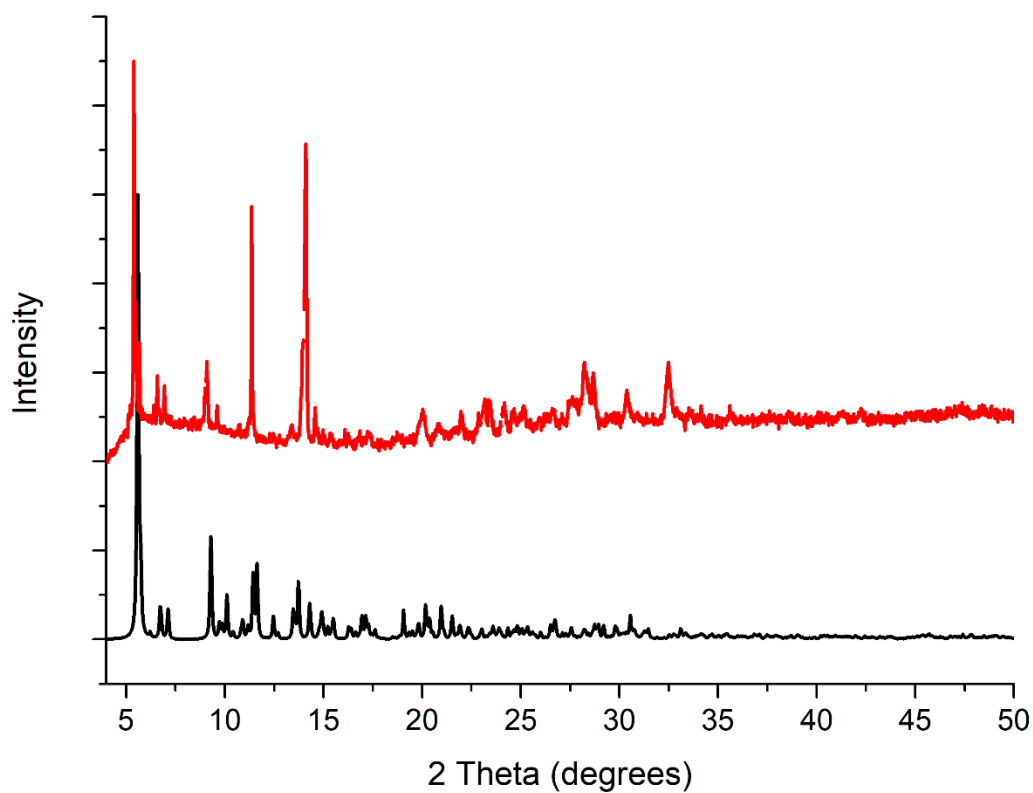


**Fig. S7** PXRD patterns of simulated (black) and as-synthesized (red) samples of **3**.

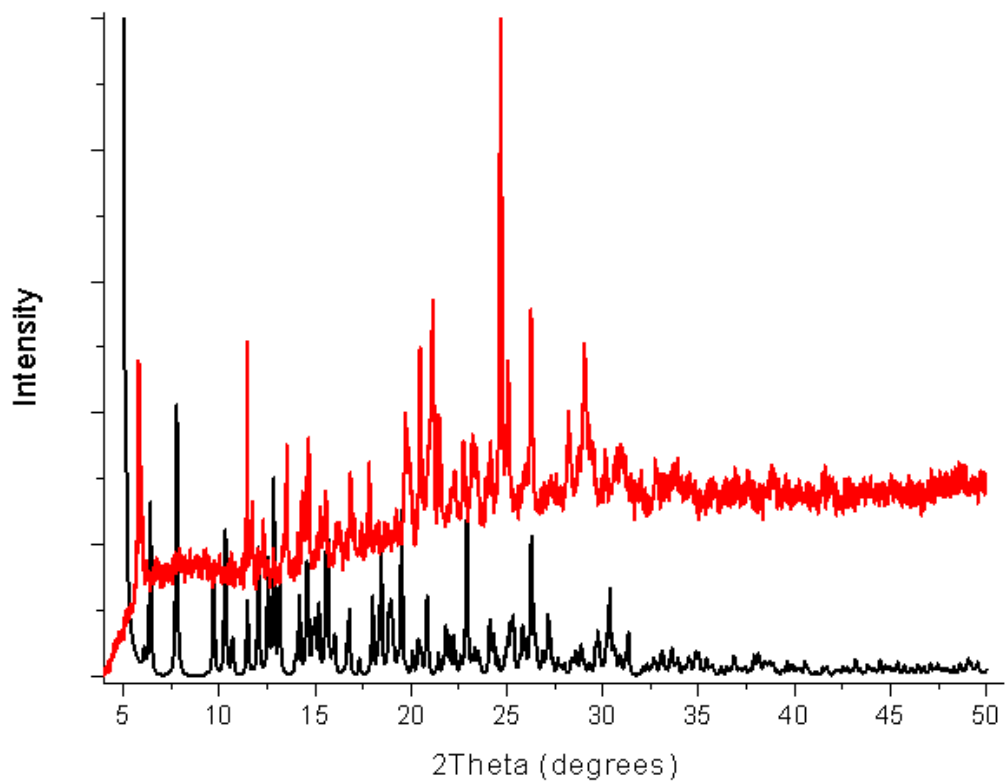


**Fig. S8** PXRD patterns of simulated (black) and as-synthesized (red) samples of **4**.

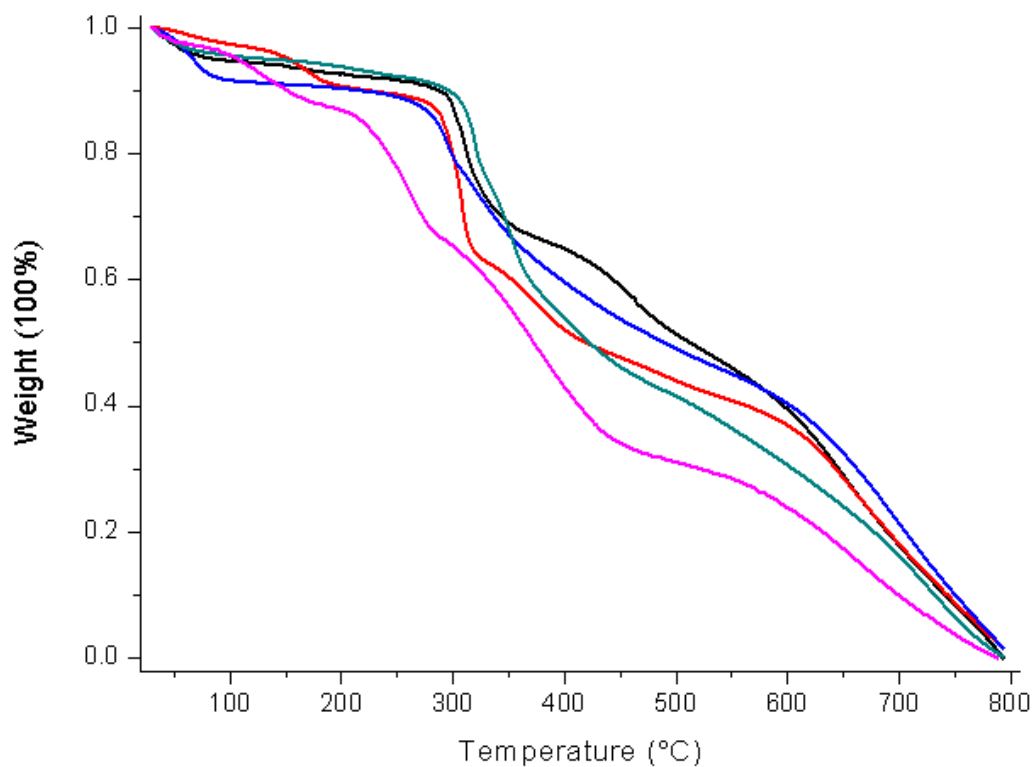


**Fig. S9** TGA plots of cage **1a** (red), **1b** (black), **2** (blue), **3** (green) and **4** (pink) measured under N<sub>2</sub> atmosphere.

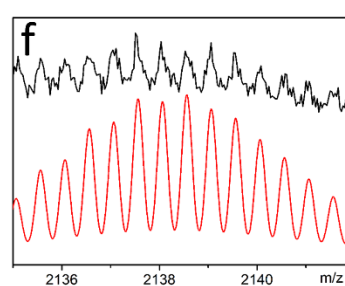
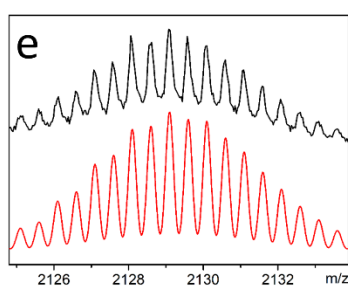
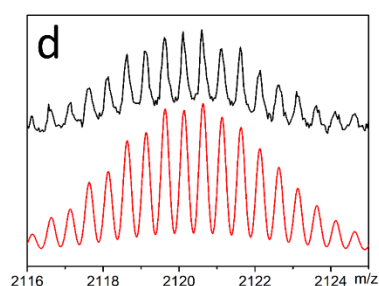
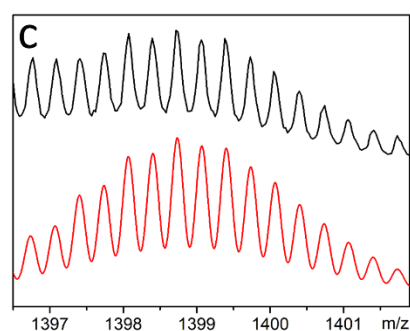
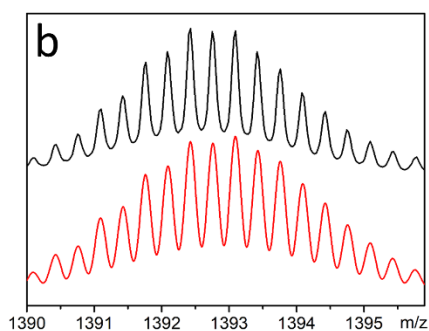
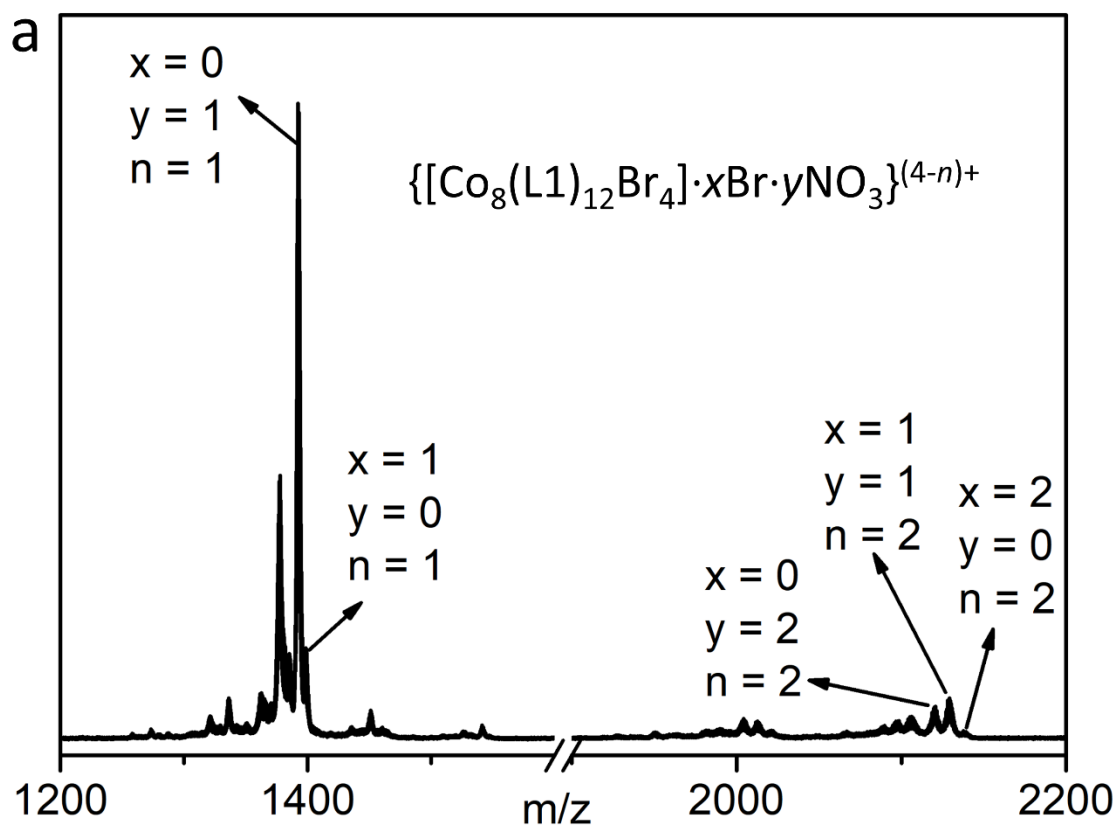


**Fig. S10** (a) The API-TOF mass spectrum of cage **1b**. The expanded spectra of  $\{[\text{Co}_8(\text{L1})_{12}\text{Br}_4] \cdot x\text{Br} \cdot y\text{NO}_3\}^{(4-n)+}$ : (b) the  $\{[\text{Co}_8(\text{L1})_{12}\text{Br}_4] \cdot \text{NO}_3\}^{3+}$  peak, (c) the  $\{[\text{Co}_8(\text{L1})_{12}\text{Br}_4] \cdot \text{Br}\}^{3+}$  peak, (d) the  $\{[\text{Co}_8(\text{L1})_{12}\text{Br}_4] \cdot 2\text{NO}_3\}^{2+}$  peak, (e) the  $\{[\text{Co}_8(\text{L1})_{12}\text{Br}_4] \cdot \text{Br} \cdot \text{NO}_3\}^{2+}$  peak, and (f)  $\{[\text{Co}_8(\text{L1})_{12}\text{Br}_4] \cdot 2\text{Br}\}^{2+}$  peak. Black: observed isotope patterns; red: simulated isotope patterns.

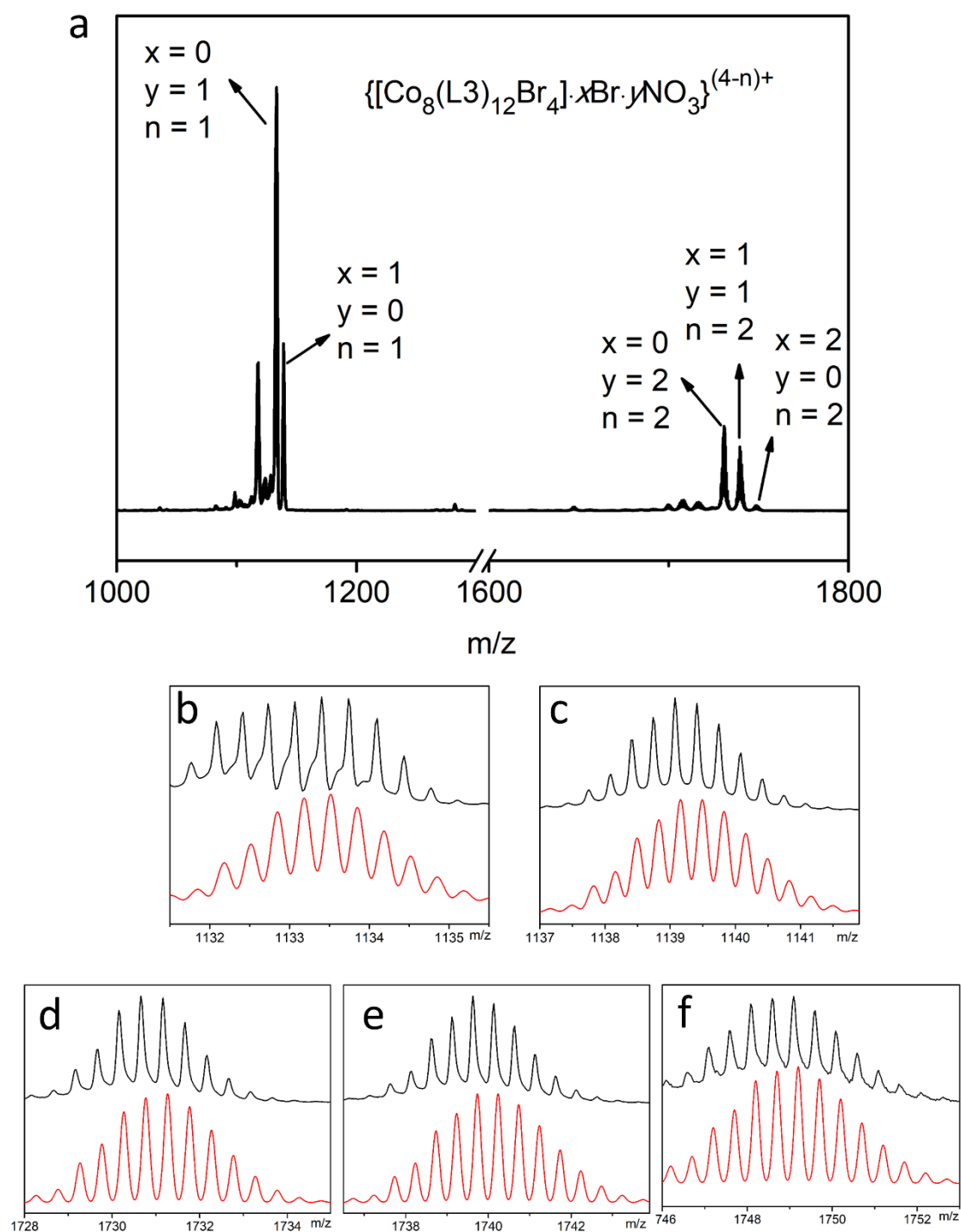


**Fig. S11** (a) The API-TOF mass spectrum of cage **3**. The expanded spectra of  $\{[\text{Co}_8(\text{L3})_{12}\text{Br}_4] \cdot x\text{Br} \cdot y\text{NO}_3\}^{(4-n)+}$ : (b) the  $\{[\text{Co}_8(\text{L3})_{12}\text{Br}_4] \cdot \text{NO}_3\}^{3+}$  peak, (c) the  $\{[\text{Co}_8(\text{L3})_{12}\text{Br}_4] \cdot \text{Br}\}^{3+}$  peak, (d) the  $\{[\text{Co}_8(\text{L3})_{12}\text{Br}_4] \cdot 2\text{NO}_3\}^{2+}$  peak, (e) the  $\{[\text{Co}_8(\text{L3})_{12}\text{Br}_4] \cdot \text{Br} \cdot \text{NO}_3\}^{2+}$  peak, and (f)  $\{[\text{Co}_8(\text{L3})_{12}\text{Br}_4] \cdot 2\text{Br}\}^{2+}$  peak. Black: observed isotope patterns; red: simulated isotope patterns.

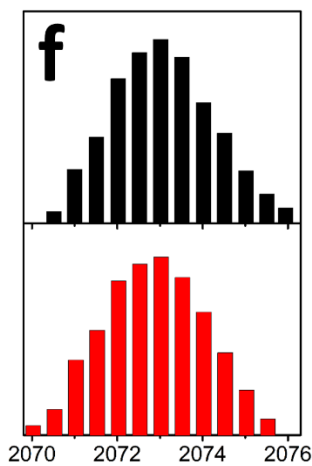
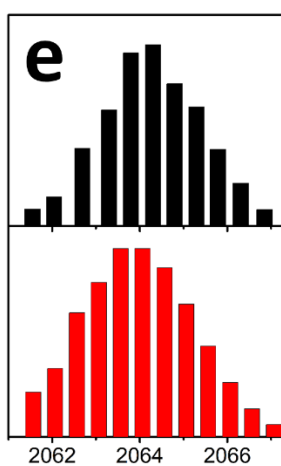
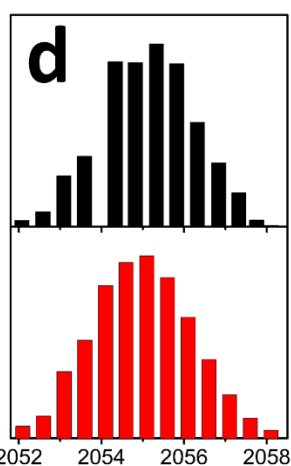
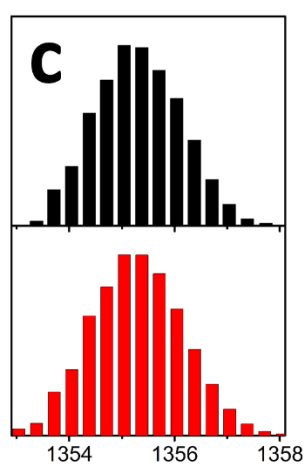
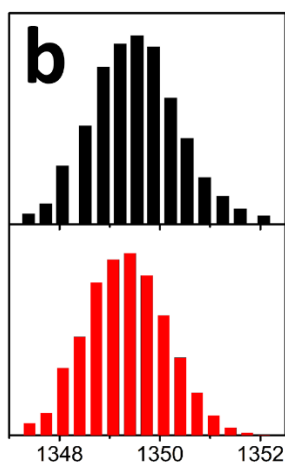
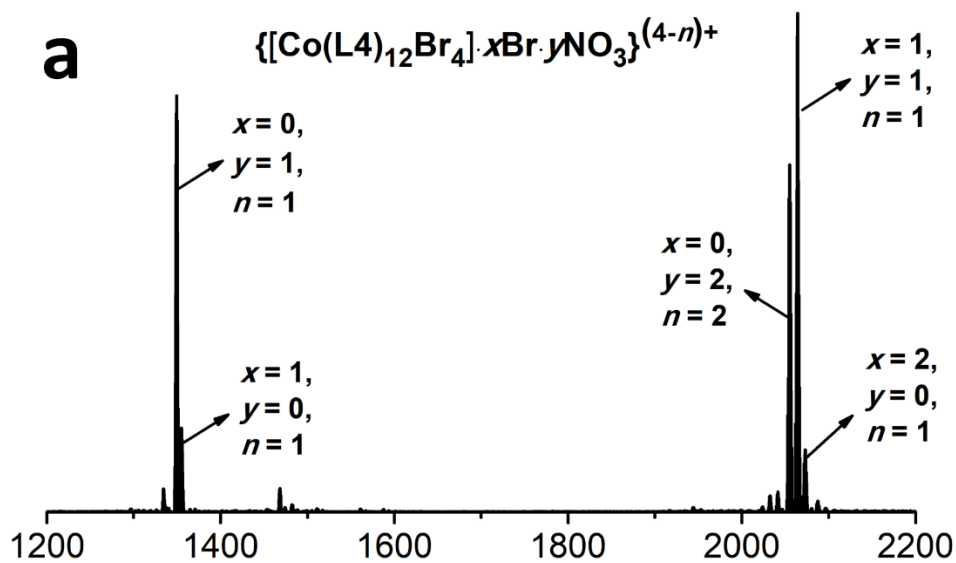


**Fig. S12** (a) The ESI-TOF mass spectrum of cage **4**. The expanded spectra of  $\{[\text{Co}_8(\text{L4})_{12}\text{Br}_4] \cdot x\text{Br} \cdot y\text{NO}_3\}^{(4-n)+}$ : (b) the  $\{[\text{Co}_8(\text{L4})_{12}\text{Br}_4] \cdot \text{NO}_3\}^{3+}$  peak, (c) the  $\{[\text{Co}_8(\text{L4})_{12}\text{Br}_4] \cdot \text{Br}\}^{3+}$  peak, (d) the  $\{[\text{Co}_8(\text{L4})_{12}\text{Br}_4] \cdot 2\text{NO}_3\}^{2+}$  peak, (e) the  $\{[\text{Co}_8(\text{L4})_{12}\text{Br}_4] \cdot \text{Br} \cdot \text{NO}_3\}^{2+}$  peak, and (f)  $\{[\text{Co}_8(\text{L4})_{12}\text{Br}_4] \cdot 2\text{Br}\}^{2+}$  peak. Black: observed isotope patterns; red: simulated isotope patterns.

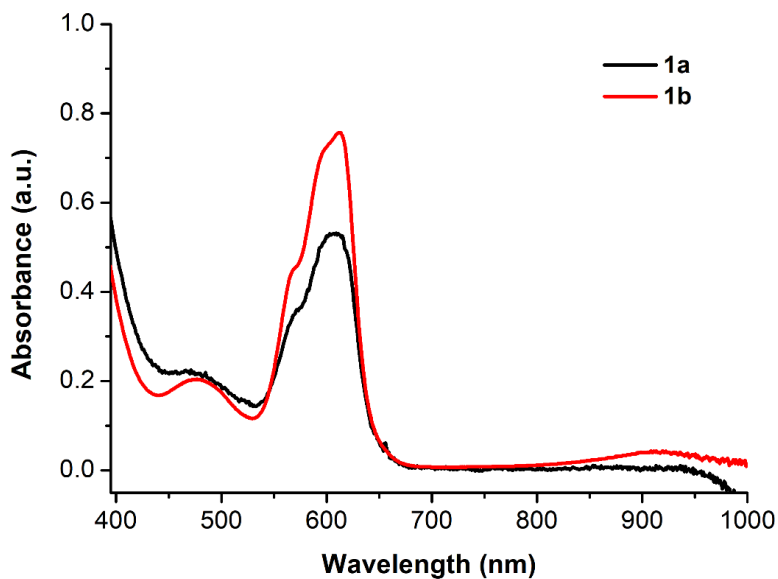


**Fig. S13** UV-Vis absorption spectra of cage **1a** and **1b** in DMF with concentration of 0.2 mmol/L.

#### Electrochemical measurements

Electrochemical measurements were performed on a CHI660E electrochemical workstation with a conventional three-electrode system consisted of a homemade Ag/AgCl electrode (soaked in saturated KCl aqueous solution) as the reference electrode, a piece of platinum silk 0.5 mm diameter as the counter electrode, and a 1.0 mm diameter glassy carbon electrode as the working electrode. The samples in spectral purity DMF solution containing 0.1 mol/L  $[n\text{-Bu}_4\text{N}][\text{PF}_6]$  as the supporting electrolyte. The measurements were performed at room temperature after the solutions were degassed with nitrogen. Reference electrode Ag/AgCl (soak in saturated KCl aqueous solution) was used as an internal standard, and all potentials are referenced to the Ag/AgCl couple at 0 V.

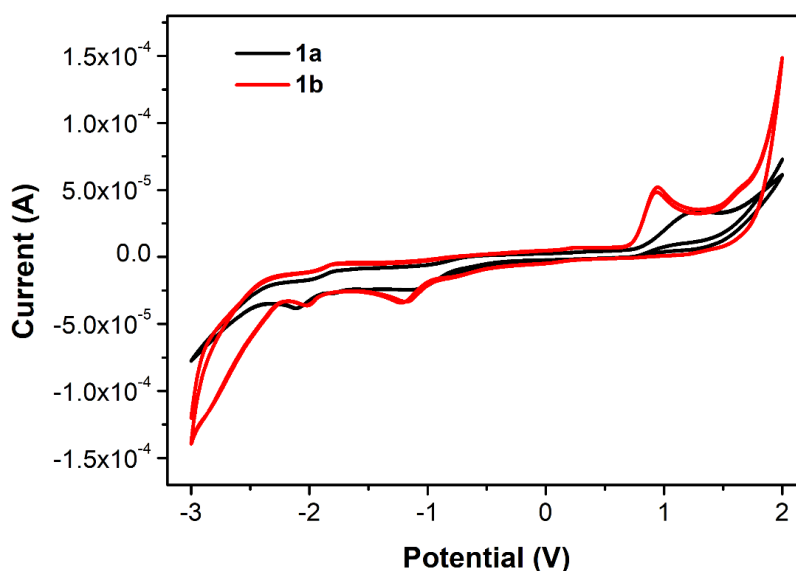


**Fig. S14** Cyclic voltammetry of **1a** and **1b**. Test condition: the CV curves were acquired by using a glassy carbon electrode (GCE) in a DMF solution of 0.1 M  $[n\text{-Bu}_4\text{N}][\text{PF}_6]$  under a nitrogen atmosphere and the Ag/AgCl couple was selected as reference for the potentials of each redox couple (scan rate at 100 mV/s).

## Magnetic property measurements

1. The molar magnetic susceptibility  $\chi_M$  can be calculated via the followed equation,

$$\chi_M = \frac{\widehat{M}}{\widehat{H} \cdot n}$$

Here  $\chi_M$  is the molar magnetic susceptibility ( $\text{cm}^3/\text{mol}$ );  $\widehat{M}$  is the magnetization ( $\text{cm}^3 \cdot \text{Oe}$ );  $\widehat{H}$  is the magnetic field strength (Oe);  $n$  is the amount of substance (mol).

2. The  $\chi_M T$  value can be calculated via the followed equation,

$$\chi_M = \frac{N g^2 \mu_B^2}{3kT} \sum S(S+1) = \frac{C}{T}$$

Here  $C$  is Curie constant;  $N\mu_B^2/3k = 0.125 \text{ cm}^3 \cdot \text{K} \cdot \text{mol}^{-1}$ ,  $C = 0.125 g^2 \sum S(S+1) = \chi_M T$  (room temperature);  $N$  is Avogadro constant =  $6.02 \times 10^{23}$ ;  $g$  is Lande factor;  $\mu_B$  is Bohr magnet =  $9.274 \times 10^{-24} \text{ J T}^{-1}$ ;  $k$  is Boltzmann constant =  $1.38 \times 10^{-23} \text{ J K}^{-1}$ ;  $T$  is temperature;  $S$  is spin quantum number;  $n$  is numbers of unpaired electrons, when we ignored orbital angular momentum contribution,

$$\mu_{eff} = \mu_B g [\sum S(S+1)]^{1/2}, \chi_M = (N\mu_{eff}^2)/3kT, \mu_{eff} = 2.83 \mu_B [\chi_M T]^{1/2}$$

$$\mu_{eff} = [3kT\chi_M/N]^{1/2} = \mu_B g [\sum S(S+1)]^{1/2} = 2.83 \mu_B [\chi_M T]^{1/2} = \mu_B [n(n+2)]^{1/2}$$

The testing weight of cage **1a** is 25.88 mg and the M.W. of complex **1a** is  $4308.02 \text{ g mol}^{-1}$ , so the amount of substance of cage **1a** is  $6.01 \times 10^{-6} \text{ mol}$ .

The testing weight of cage **1b** is 27.26 mg and the M.W. of complex **1b** is  $4609.74 \text{ g mol}^{-1}$ , so the amount of substance of cage **1b** is  $5.91 \times 10^{-6} \text{ mol}$ .

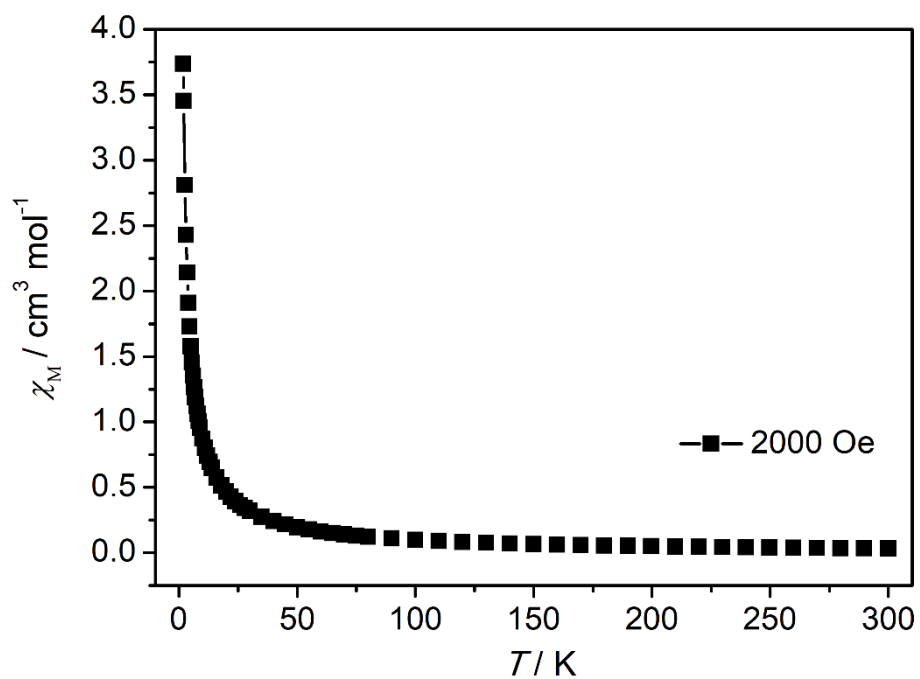


**Fig. S15** The temperature dependence of molar magnetic susceptibility for complex **1a** obtained at 2000 Oe field (plot of  $\chi_M$  versus T).

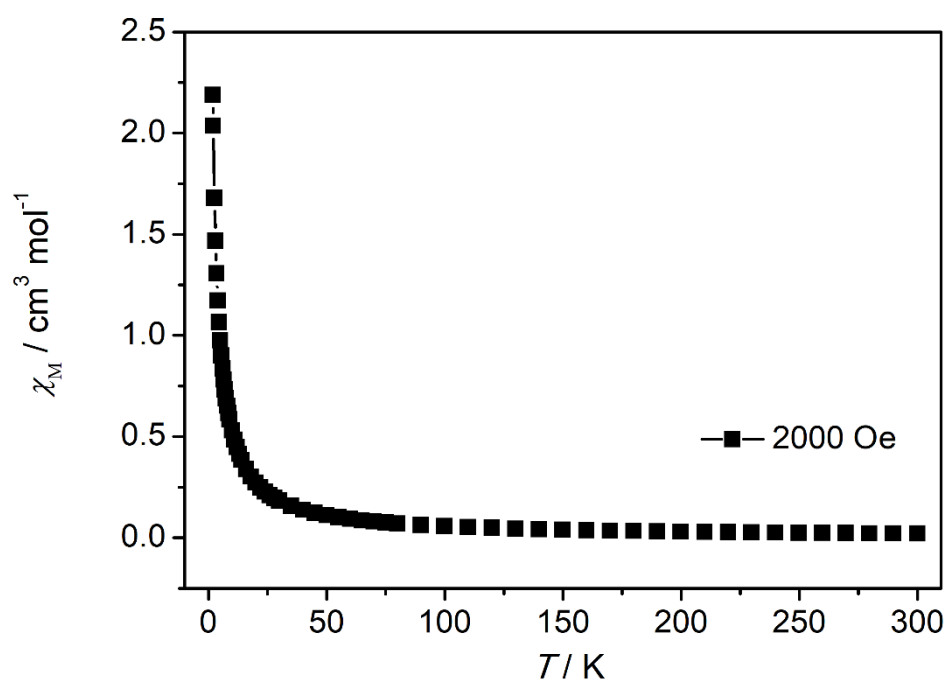


**Fig. S16** The temperature dependence of molar magnetic susceptibility for complex **1b** obtained at 2000 Oe field (plot of  $\chi_M$  versus T).

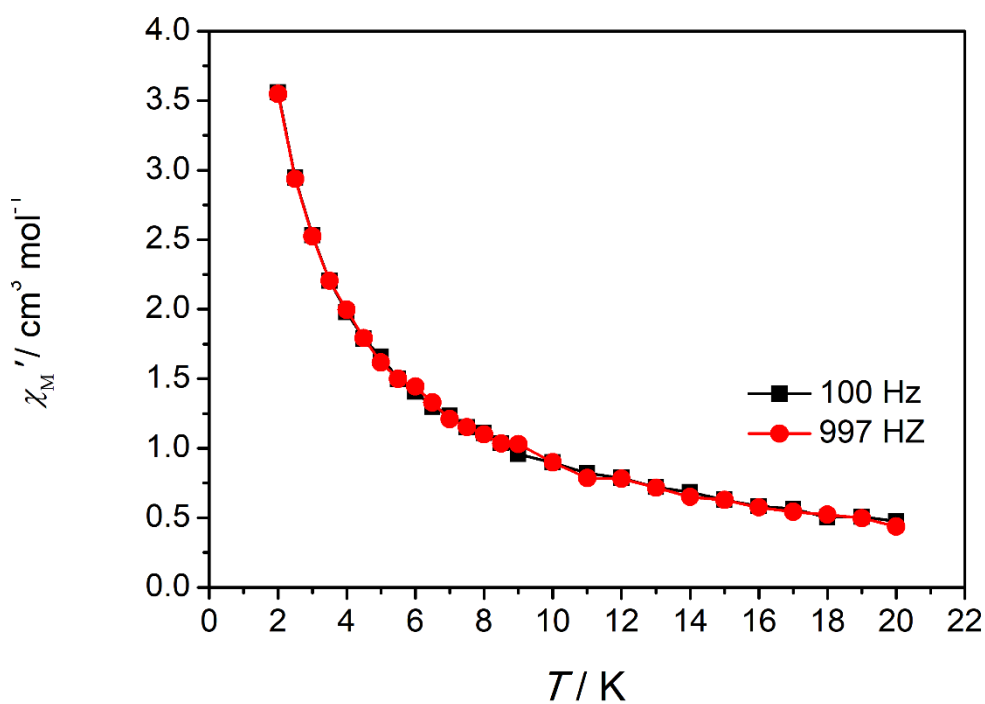


**Fig. S17** The temperature dependence of ac magnetic susceptibility  $\chi'_M$  (in-phase) for complex **1a** obtained at zero magnetic field under 100 Hz (black) and 997 Hz (red). (plots of  $\chi'_M$  versus T)

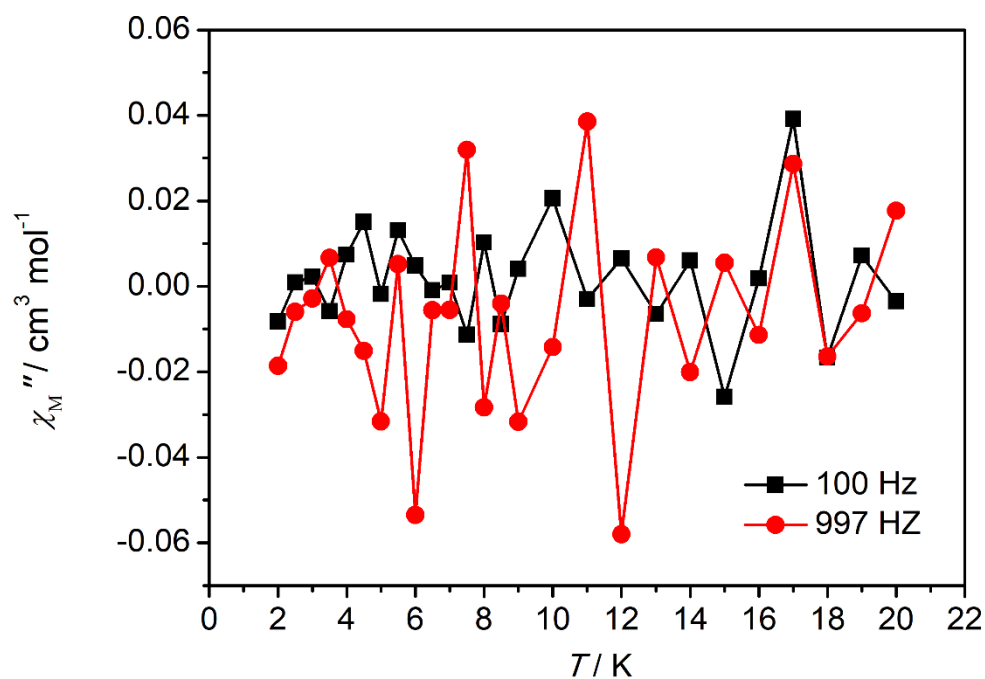


**Fig. S18** The temperature dependence of ac magnetic susceptibility  $\chi''_M$  (out-of-phase) for complex **1a** obtained at zero magnetic field under 100 Hz (black) and 997 Hz (red). (plots of  $\chi''_M$  versus T)

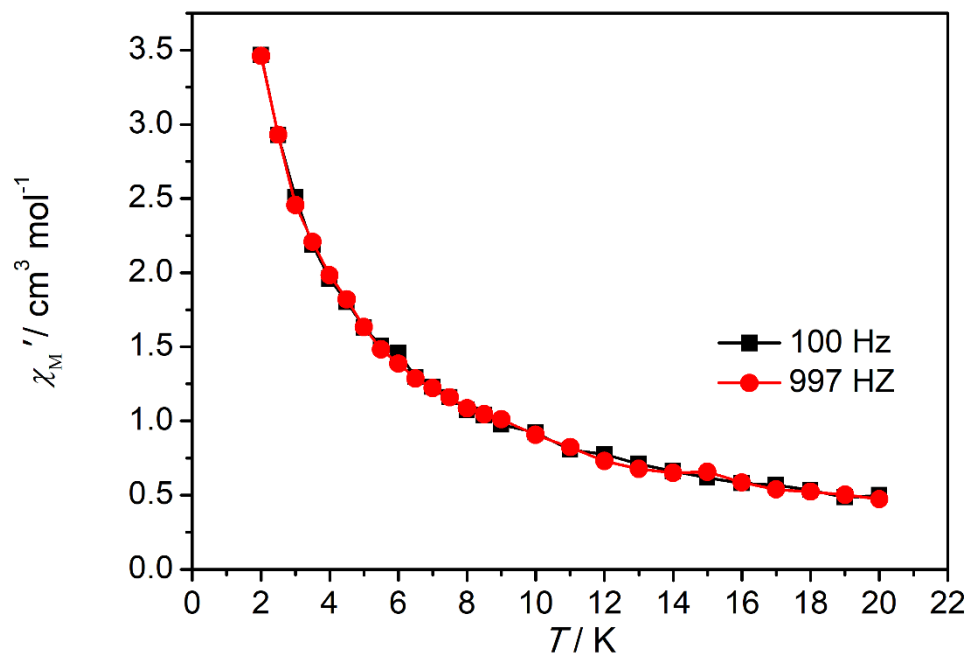


**Fig. S19** The temperature dependence of ac magnetic susceptibility  $\chi'_M$  (in-phase) for complex **1a** obtained at 1000 Oe field under 100 Hz (black) and 997 Hz (red). (plots of  $\chi'_M$  versus T)

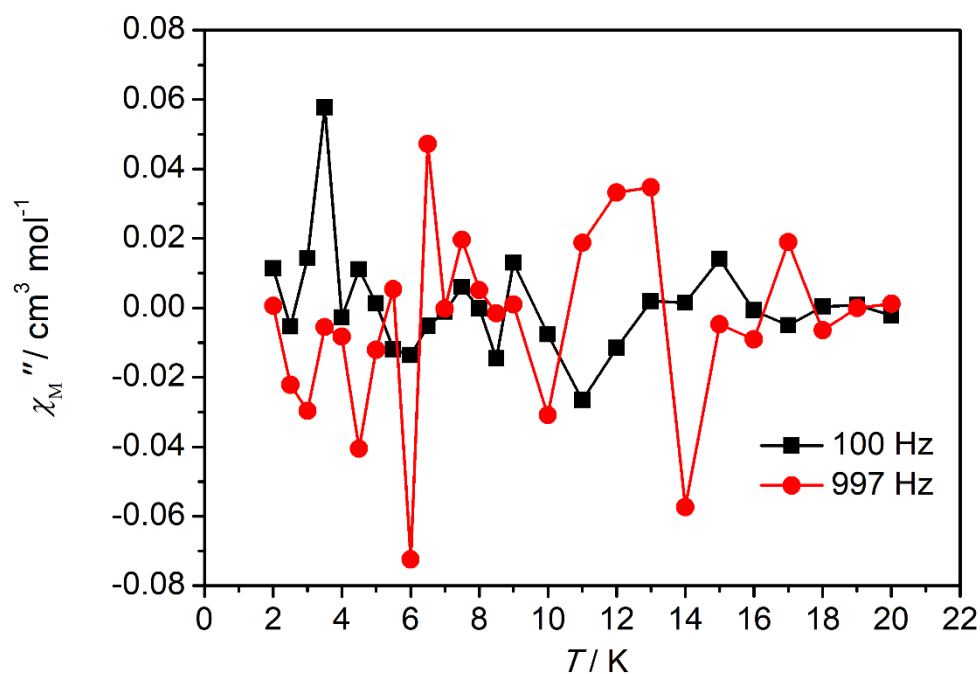


**Fig. S20** The temperature dependence of ac magnetic susceptibility  $\chi''_M$  (out-of-phase) for complex **1a** obtained at 1000 Oe field under 100 Hz (black) and 997 Hz (red). (plots of  $\chi''_M$  versus T)

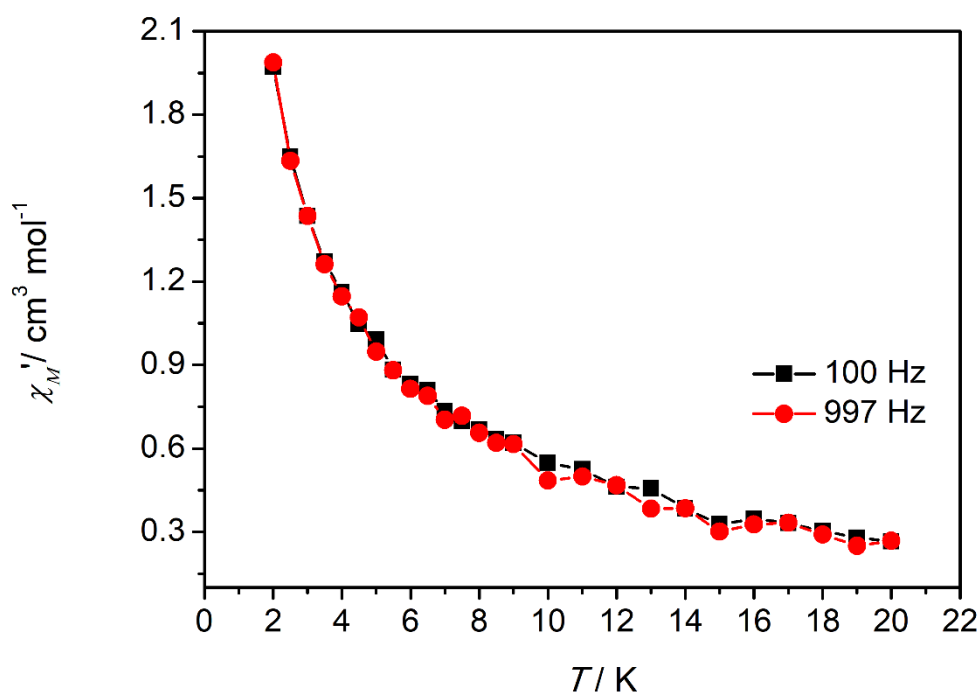


**Fig. S21** The temperature dependence of ac magnetic susceptibility  $\chi'_M$  (in-phase) for complex **1b** obtained at zero magnetic field under 100 Hz (black) and 997 Hz (red). (plots of  $\chi'_M$  versus T)

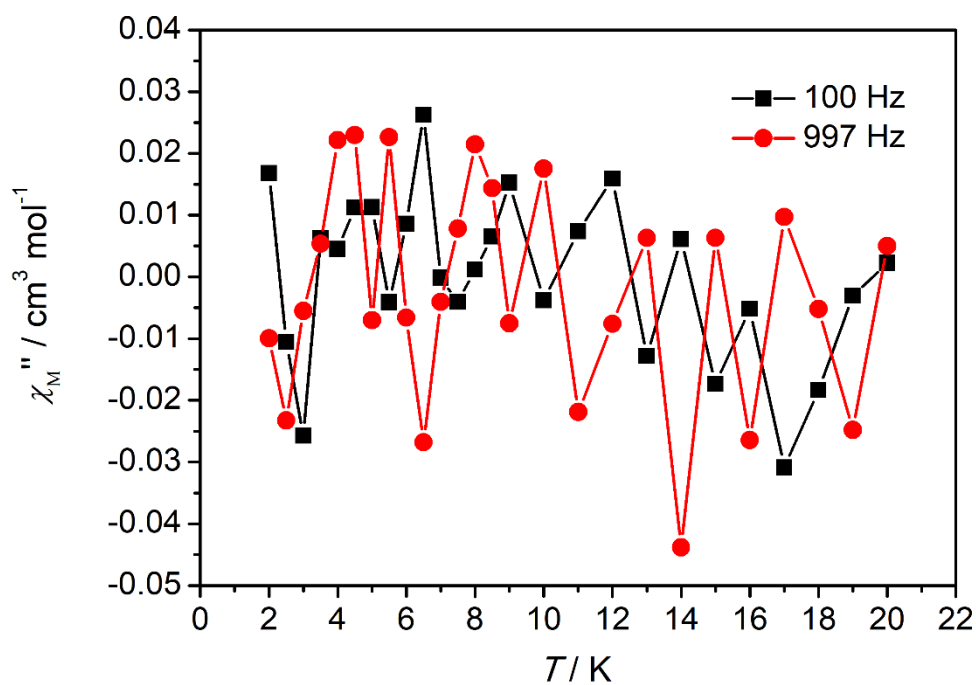


**Fig. S22** The temperature dependence of ac magnetic susceptibility  $\chi''_M$  (out-of-phase) for complex **1b** obtained at zero magnetic field under 100 Hz (black) and 997 Hz (red). (plots of  $\chi''_M$  versus T)

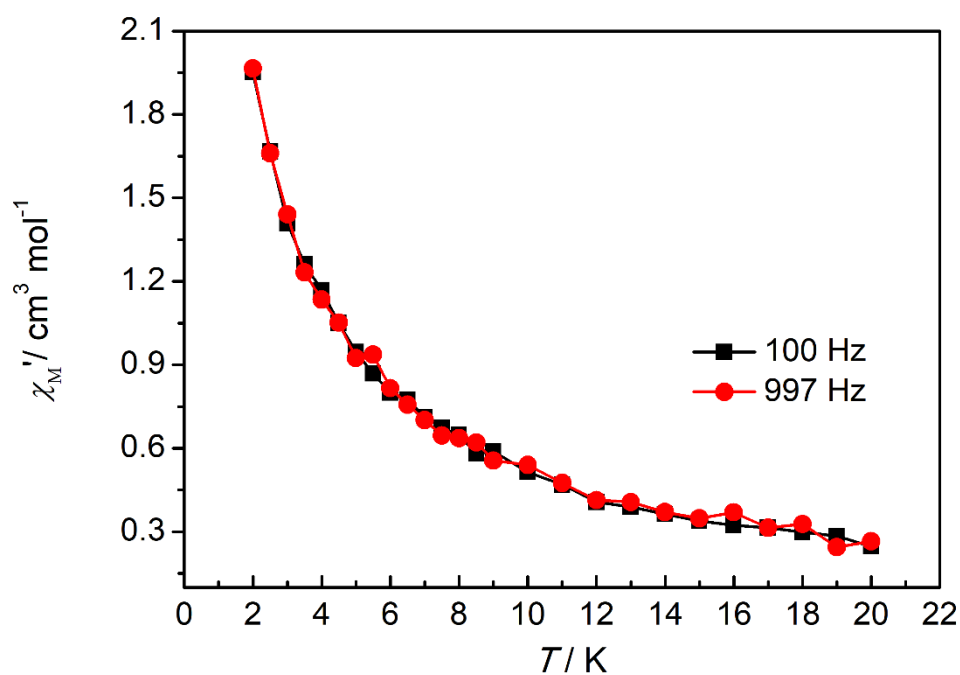


**Fig. S23** The temperature dependence of ac magnetic susceptibility  $\chi'_M$  (in-phase) for complex **1b** obtained at 1000 Oe field under 100 Hz (black) and 997 Hz (red). (plots of  $\chi'_M$  versus T)

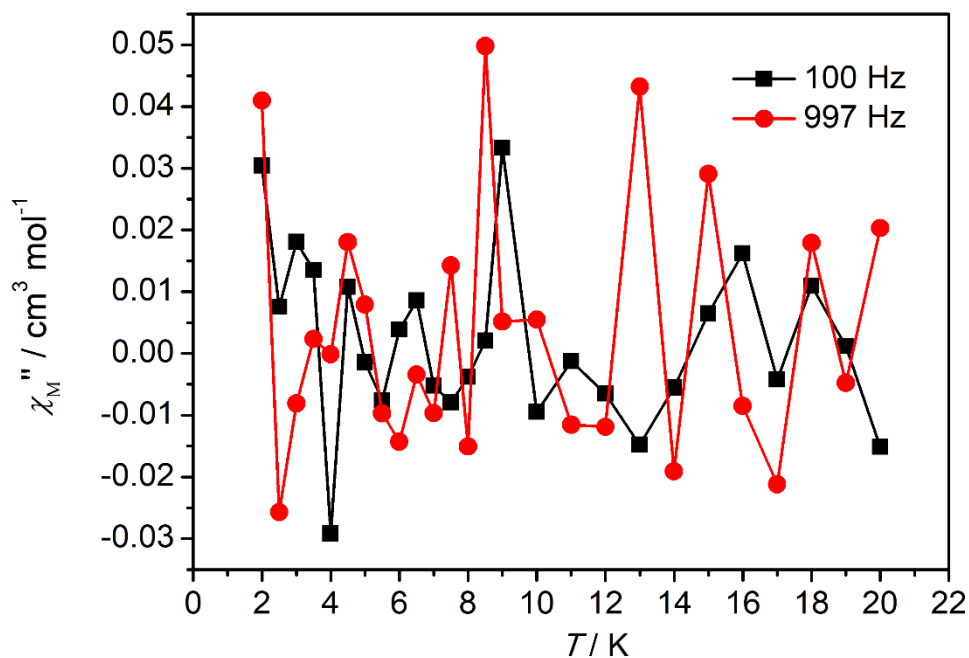


**Fig. S24** The temperature dependence of ac magnetic susceptibility  $\chi''_M$  (out-of-phase) for complex **1b** obtained at 1000 Oe field under 100 Hz (black) and 997 Hz (red). (plots of  $\chi''_M$  versus T)